

Reduction of conductance-based neuron models

Thomas B. Kepler¹, L. F. Abbott², and Eve Marder¹

¹ Departments of Biology and ² Department of Physics and The Center for Complex Systems, Brandeis University, Waltham, MA 02254, USA

Received August 2, 1991/Accepted in revised form November 6, 1991

Abstract. We present a scheme for systematically reducing the number of differential equations required for biophysically realistic neuron models. The techniques are general, are designed to be applicable to a large set of such models and retain in the reduced system as high a degree of fidelity to the original system as possible. As examples, we provide reductions of the Hodgkin–Huxley system and the A-current model of Connor et al. (1977).

1 Introduction

Computational neuroscientists always face a difficult task in choosing the kind of model with which to approach a given problem. On the one hand are conductance-based models such as those epitomized by the seminal work of Hodgkin and Huxley (1952) that seek to reproduce physiological data with mathematical representations that can provide insight into the underlying biophysical mechanisms. The difficulty of developing and analyzing this kind of model has increased, as we now know that many neurons contain a large number of different voltage-dependent conductances (e.g., Yamada et al. 1989; Buchholtz et al. 1992; Golowasch et al. 1992). On the other hand we have abstract models such as those used by McCulloch and Pitts (1943); Hopfield (1982); FitzHugh (1961); and Lopicque (1907), which are mathematically and conceptually simple, although their parameters may bear no direct relationship to those of biological neurons. Indeed, despite the attractiveness of simple neuronal “caricatures” care must be exerted lest one is drawn to unwarranted conclusions based on the behavior of these abstract models.

Our aim is to provide methods that allow us to start with data-derived conductance-based models of the Hodgkin–Huxley type, and reduce these to the simplicity of neuronal caricatures while preserving a direct relationship between the parameters measured experimentally and the parameters in the simpler neuronal caricature. This will allow the modeler to use the simpler

form for analysis without losing the ability to relate the results of the analysis to the currents that produced the model.

We present a change of variables and perturbation analysis that provide a power-series approximation of the original system whose leading term is a reduced system with fewer differential equations. There are basically two techniques. One, based on singular perturbation theory, is the elimination of “fast” variables by combining them with the membrane potential to form a single variable. The second technique is the combination of variables evolving on similar time scales and having similar effects.

Previous reduction schemes for the Hodgkin–Huxley system (HH) have exploited the rapidity of sodium current activation to eliminate the sodium activation as a dynamic variable. Our analysis goes one step further by including higher-order effects of this reduction. The similar time scales of the sodium inactivation h and potassium activation n have been used to combine h and n into a single “recovery” variable. Our treatment of these techniques is intended to improve upon prior work (FitzHugh 1961; Krinskii and Kokoz 1973; Hindmarsh and Rose 1982; Rinzel 1985; Rose and Hindmarsh 1989) in two ways. First, we enhance the fidelity to the original system as much as possible, and second, we provide a systematic “recipe” which may be applied to any system with the appropriate characteristics.

In order to provide concrete examples of our method we will use HH, and a modification of HH to which the A current has been added (Connor et al. 1977). These reductions will be used to illustrate the advantages conferred by a visualizable configuration space in the analysis of several familiar phenomena.

2 Equivalent potentials

Dynamical systems that describe isopotential excitable neural membranes typically consist of two parts. The first is a differential equation expressing current conservation

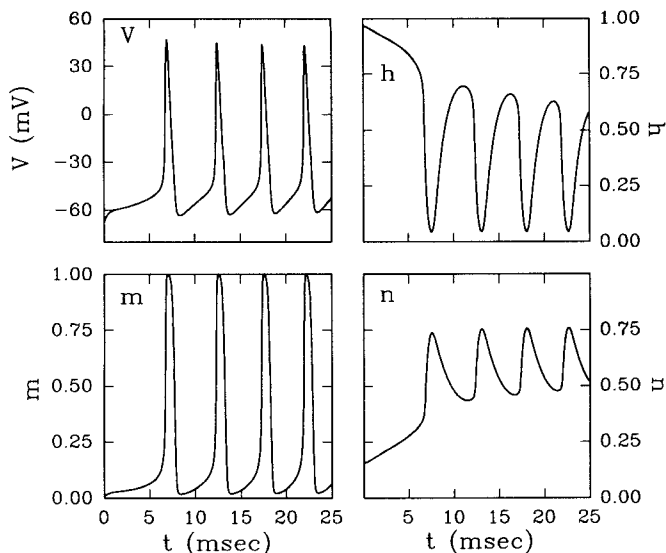


Fig. 1. Behavior of the Hodgkin-Huxley (HH) dynamical variables exhibiting repetitive spiking behavior during application of a ramped depolarizing external current. For the sake of comparison, the HH system used here is as modified by Connor et al. (1977). The models called "HH" have $\bar{g}_A = 0$ and the leak reversal potential is adjusted to give a resting potential of -68 mV

$$C \frac{dV}{dt} + I(V, \{x_i\}) = I_{\text{external}}(t)$$

where V is the membrane potential, C is the membrane capacitance and $I(V, \{x_i\})$ is the total ionic current expressed as a function of V and the gating variables x_i . Each member of the system of equations describing the dynamics of these gating variables has the form

$$\frac{dx_i}{dt} = k_i(V)[\bar{x}_i(V) - x_i],$$

providing the balance of the system's description. In the HH system, for example, the gating variables are the sodium activation variable m , the sodium inactivation variable h , and the potassium activation variable n .¹ In this system, the current $I(V, m, h, n)$ is

$$I(V, m, h, n) = \bar{g}_{\text{Na}} m^3 h (V - E_{\text{Na}}) + \bar{g}_{\text{K}} n^4 (V - E_{\text{K}}) + g_{\text{leak}} (V - E_{\text{leak}})$$

where \bar{g}_{carrier} is the maximum conductance for that carrier, and E_{carrier} is its reversal potential. Figure 1 shows repetitive firing of the HH system under ramped current injection. We have plotted V , m , h and n each against time.

To combine different variables together for the purpose of reduction, it helps to make them dimensionally

¹ A more familiar form of the equations governing the evolution of HH gating variables is, in the case of m ,

$$dm/dt = \alpha_m(V)(1 - m) - \beta_m(V)m$$

and is related to ours through $k_m(V) = \alpha_m(V) + \beta_m(V)$ and $k_m(V)\bar{m}(V) = \alpha_m(V)$

equivalent. The membrane potential is ubiquitous in this system, entering the equations for each of the other variables, providing the sole link between these degrees of freedom and is, moreover, the sole mediator of external information to the system. This suggests that all the other variables might profitably be converted to *equivalent potentials*, defined for each of the gating variables as the potential v_i which makes $\bar{x}_i(v_i) = x_i$:

$$v_i = \bar{x}_i^{-1}(x_i)$$

where the exponent -1 refers to the functional inverse. In other words, the equivalent potential is the voltage which, in voltage clamp, would give the value x_i to the i th gating variable after equilibrium is reached. Note that equivalent potentials provide as complete and valid a description of the system as the gating variables. The equilibrium (and hence static) relationship used to define them does not compromise their dynamic variability in any way. The transformation requires that the functions \bar{x} are invertible. The class of models that we are considering does not include those that contain calcium-dependent conductances, since in these, some of the \bar{x} depend both on the membrane potential and on the calcium concentration. Further work may be required to reduce those variables that depend on the calcium concentration.

The chain rule may be applied to give us new equations of motion expressed in terms of the equivalent potentials:

$$C \frac{dV}{dt} + F(V, \{v_i\}) = I_{\text{external}}(t)$$

where

$$F(V, \{v_i\}) \equiv I(V, \{\bar{x}_i(v_i)\}),$$

and

$$\begin{aligned} \frac{dv_i}{dt} &= \frac{k_i(V)}{\bar{x}'_i(v_i)} [\bar{x}_i(V) - \bar{x}_i(v_i)] \\ &\equiv f_i(V, v_i) \end{aligned} \quad (1)$$

and the prime denotes differentiation. Note that for these variables, all of the surfaces on which the time derivatives of (1) vanish (its nullclines) are simply hypersurfaces given by $v_i = V$, so that at equilibrium all of the equivalent potentials equal the (true) membrane potential. The only non-trivial nullcline is that for the current conservation equation. No approximations have yet been made; the new system is entirely equivalent to the original.

The evolution of the whole HH system expressed in equivalent potentials is shown in Fig. 2. The transformation to equivalent potentials reveals that of the four available degrees of freedom, only two are effectively utilized: v_m is nearly indistinguishable from V ; likewise with v_h and v_n . The motions of the system within the four-dimensional configuration space are largely confined to a two-dimensional submanifold. Moreover we have at hand a convenient way of locating this manifold and formulating the appropriate dynamics on

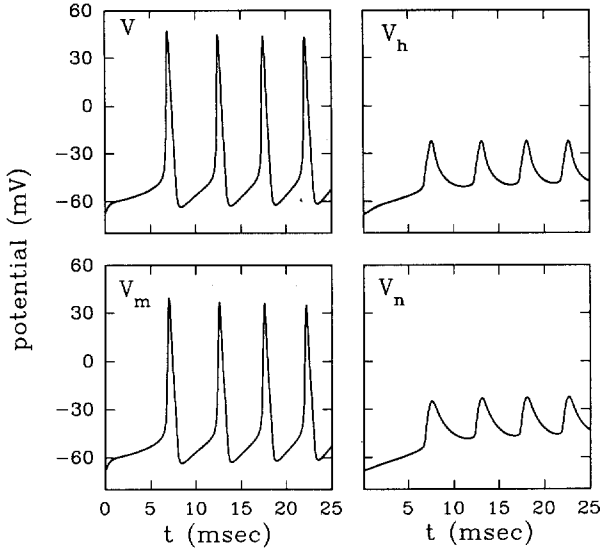


Fig. 2. Behavior of the same system as in Fig. 1 expressed in equivalent potentials. Note that the trajectories for V and v_m and for v_h and v_n are similar suggesting that a reduction to two variables is possible

it: we will form averages and differences of equivalent potentials within the two sets.

3 Perturbation series

In the general case, the equivalent potentials will fall naturally into two or more groups. One group will contain the true membrane potential V . We will assume that there is only one other group, but this is merely a convenience, since operations on distinct groups do not interfere. Suppose that the first group contains N_1 variables and the second contains N_2 . We will distinguish members of the two groups by using Greek indices μ, ν , etc., which will take values 0 through $N_1 - 1$, for the first group, and for the second, Latin indices i, j , etc., taking values N_1 through $N_1 + N_2$. We will refer to V as v_0 when convenient. Within each group we make a change of variables to 1) a new *representative* equivalent potential taken as a weighted average over all members of the group, and 2) differences between each member and their average. The transformations are

$$\varphi = \sum_{\mu} \alpha_{\mu} v_{\mu} \quad \psi = \sum_i \alpha_i v_i \quad (2)$$

and

$$v_{\mu} = \varphi + \delta_{\mu} \quad v_i = \psi + \delta_i. \quad (3)$$

We constrain the α_i and the α_{μ} (separately) to sum to one, and the sums of the products $\alpha_{\mu} \delta_{\mu}$ and $\alpha_i \delta_i$ to vanish. In addition, we intend that the α_i and the α_{μ} should be positive. This will impose a condition on the applicability of the reduction scheme. Our job is to pick the α 's to optimize the agreement between the full and reduced models. Our strategy will be to operate locally,

in the vicinity of the equilibrium point, rather than globally, since global constraints do not readily yield closed solutions. The reduced system will then have exactly the right value of the equilibrium potential at all values of external current and very nearly the correct stability and bifurcation characteristics.

We can differentiate (2), use (3), and expand to first order in the δ 's to get

$$\frac{d\psi}{dt} = \sum_i \alpha_i f_i(\varphi, \psi) + \delta_0 \sum_i \alpha_i \frac{\partial f_i}{\partial v_0} + \sum_i \delta_i \alpha_i \frac{\partial f_i}{\partial v_i} + O(\delta^2) \quad (4)$$

and

$$C \frac{d\varphi}{dt} + \alpha_0 F(\varphi, \psi) + \alpha_0 \sum_i \delta_i \frac{\partial F}{\partial v_i} + \delta_0 \left(\alpha_0 \frac{\partial F}{\partial v_0} - C \sum_{\mu \neq 0} \alpha_{\mu} k_{\mu} \right) + \sum_{\mu \neq 0} \delta_{\mu} \left(\alpha_{\mu} \frac{\partial F}{\partial v_{\mu}} + C \alpha_{\mu} k_{\mu} \right) + O(\delta^2) = \alpha_0 I_{\text{external}}(t). \quad (5)$$

Here and in the following we adopted the convention that functions without explicit arguments are to be evaluated at $v_{\mu} = \varphi$ and $v_i = \psi$ for all μ and i . Note that in (5) a term $C \sum_{\mu} \alpha_{\mu} f_{\mu}(\varphi, \varphi)$ has been omitted since $f_{\mu}(\varphi, \varphi) = 0$ for each μ , and we have used $-\partial f_{\mu} / \partial v_{\mu}|_{\varphi, \varphi} = \partial f_{\mu} / \partial v_0|_{\varphi, \varphi} = k_{\mu}$.

Recall that the δ 's are not independent. We account for this by adding to (4) and (5) Lagrange multiplier terms to impose the constraints that the sums of the products $\alpha_{\mu} \delta_{\mu}$ and $\alpha_i \delta_i$ vanish. Specifically, we add

$$\lambda_1 \sum_i \alpha_i \delta_i + \lambda_2 \sum_{\mu} \alpha_{\mu} \delta_{\mu}$$

to (5) and similarly, to (4),

$$\lambda_3 \sum_i \alpha_i \delta_i + \lambda_4 \sum_{\mu} \alpha_{\mu} \delta_{\mu}.$$

We shall optimize the expansion by making the coefficients of the first-order corrections vanish so that the expansion is valid to *second* order, at least near the equilibrium point. This imposes two conditions for each potential, i.e., the coefficients of the δ_{μ} and δ_i in (4) and (5) with the Lagrange multiplier terms added should vanish. However, this is twice as many conditions as there are free variables. We will determine the α_i by requiring that the coefficients of δ_i vanish in (5) with the first line of Lagrange multiplier terms above added to it. We then determine the α_{μ} by requiring the coefficient of δ_{μ} in the same equation to vanish. This leaves the corrections proportional to δ_{μ} and δ_i in (4) with the second set of Lagrange multiplier terms added. These must be small in order for the reduction scheme to work and we impose the requirement that the coefficients of these terms are small as a consistency condition of the method.

Requiring the vanishing of the coefficient of δ_i in (5) with the additional Lagrange multiplier term gives us

$$\alpha_0 \frac{\partial F}{\partial v_i} + \lambda_1 \alpha_i = 0.$$

λ_i may be eliminated by summing this equation on i to get

$$\alpha_i = \frac{\partial F}{\partial v_i} \left[\sum_j \frac{\partial F}{\partial v_j} \right]^{-1}. \quad (6)$$

As required, this expression obeys $\sum_i \alpha_i = 1$. Requiring that the coefficient of δ_μ in the same equation vanishes, we find, after elimination of the Lagrange multiplier,

$$\alpha_0^2 \sum_\mu \frac{\partial F}{\partial v_\mu} - \alpha_0 \frac{\partial F}{\partial v_0} + C \sum_{\mu \neq 0} \alpha_\mu k_\mu = 0 \quad (7)$$

and

$$\alpha_0 \alpha_\mu \sum_v \frac{\partial F}{\partial v_v} - \alpha_0 \frac{\partial F}{\partial v_\mu} - C \alpha_\mu k_\mu = 0 \quad (\mu \neq 0). \quad (8)$$

By summing (8) on μ and adding it to (7) we see that $\sum_\mu \alpha_\mu = 1$. Equation (8) can be solved for each α_μ in terms of α_0 , and then using (7), α_0 can be written as the root of a polynomial of order N_1 , the number of equivalent potentials being averaged to form φ :

$$\alpha_0 \sum_\mu \frac{\partial F}{\partial v_\mu} - \frac{\partial F}{\partial v_0} - C \sum_{\mu \neq 0} k_\mu \frac{\partial F}{\partial v_\mu} \left[C k_\mu - \alpha_0 \sum_v \frac{\partial F}{\partial v_v} \right]^{-1} = 0. \quad (9)$$

The appropriate root of this equation is determined by the requirement that α_0 goes to one in the limit when all the rate constants k_μ go to infinity.

We have thus far assumed that the α 's are constant. The expressions we have derived for them, however, specify them as functions of φ and ψ . We have either to pick fixed values of φ and ψ at which to evaluate these functions, or allow them to have the voltage dependence given by (6) and (9). In either case, our goals will not strictly be met, but the latter choice has the advantage of working equally well for all values of external current. Furthermore, one can see that the remnant first-order terms introduced through the time derivatives of the α 's vanish at the equilibrium point, so that while our expansion is not second-order exact everywhere, it is second-order exact in the neighborhood of an equilibrium point. (Expand the derivatives as $d\alpha/dt = \partial\alpha/\partial\varphi d\varphi/dt + \partial\alpha/\partial\psi d\psi/dt$. The terms $d\varphi/dt$ and $d\psi/dt$ vanish at equilibrium.) We have found empirically that this choice yields very good results, even far from equilibrium.

In order for this scheme to be consistent we must similarly require that the first-order correction terms in (4) (with Lagrange multiplier terms included) are small. There are two sets of first-order terms, those multiplied by δ_i and those proportional to δ_μ . Putting in the value of the Lagrange multiplier, the coefficient of the δ_i correction is

$$\frac{\partial f_i}{\partial v_i} - \sum_j \alpha_j \frac{\partial f_j}{\partial v_j}.$$

We are primarily interested in evaluating this at equilibrium, where $\partial f_i/\partial v_i = -k_i$. We normalize by dividing by $\sum_i k_i$ to get the first condition required for the corrections to the reduction to be small,

$$\left| \sum_j \alpha_j k_j - k_i \left[\sum_j k_j \right]^{-1} \right| \ll 1 \quad (10)$$

with α_i given by (6). Note that the left side of the inequality 10 vanishes identically if all the k_i are equal. Similar k values within a reduced group is one of the conditions mentioned in the introduction and may be viewed as one of the presuppositions of the reduction scheme.

A second consistency condition comes from demanding the smallness of the coefficient of the δ_μ in (4) with Lagrange multiplier terms added. This requires that all the α_μ for $\mu \neq 0$ are small, which from the constraint that the α 's sum to one means that α_0 is close to one. From (8) this gives the condition

$$\left| \frac{1}{C k_\mu} \frac{\partial F}{\partial v_\mu} \right| \ll 1 \quad (11)$$

for each $\mu \neq 0$. This, too, is an expected precondition for the applicability of the reduction procedure. The derivative in the above equation can be interpreted as the conductance associated with a given equivalent potential. Then C divided by this conductance is just an effective membrane time constant corresponding to the equivalent potential and the above condition states that rate constant k_μ must be greater than one over this time constant. In the limit as $k_\mu \rightarrow \infty$, we recover the ordinary singular perturbation solution.

Note that (6) and (8) provide us with one further check on the soundness of the reduction. We have not yet imposed the requirement that the α 's are positive. In particular, if some of the α 's are negative, the denominator in (6) could vanish. At such a singularity, the equilibrium point can switch from being attractive to being repulsive. This occurs when the equivalent potentials involved are antisynergistic, i.e., have opposite effect on the membrane current. For example, in the Hodgkin-Huxley reduction h and n can be combined not simply because the equivalent potentials of h and n are very similar, but because $\text{sign}(\bar{n}' \partial I / \partial n) = \text{sign}(\bar{h}' \partial I / \partial h)$, that is, \bar{n} increases ($\bar{n}' > 0$) and h inactivates an inward current ($\partial I / \partial h < 0$). Thus the clustering of variables into groups should be based on sharing both a common time scale and a common sign of influence on the ionic current. These groups may then be replaced by representative equivalent potentials with the procedures spelled out above.

Similarly, the weights α_μ should be positive. From (8) this means that we must require $\partial F / \partial v_\mu < 0$ for all μ . This in turn assures that the denominator in (9) will not vanish. The condition $\partial F / \partial v_\mu < 0$ means that the equivalent potential v_μ must correspond to the activation of an inward current (like the m variable of HH) or the inactivation of an outward current.

Note that if a gating process does not contribute to the ionic current, for example, if the maximum conductance for the current that involves that process is set to zero, then the associated equivalent potential has weight zero toward the construction of either ψ or φ , as should be.

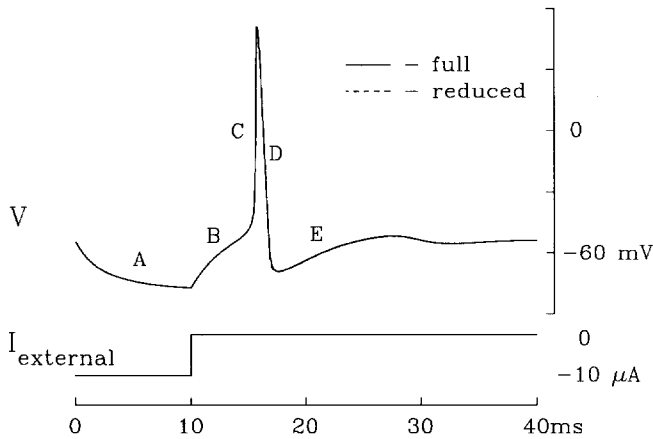


Fig. 3. The phenomenon of post-inhibitory rebound. Hyperpolarizing current is applied to the HH model and then released. A single action potential fires before the system settles down to rest. Traces from the full model (solid line) and the reduced model (dashed line) are overlaid. Alphabetic labels are for comparison with Fig. 4

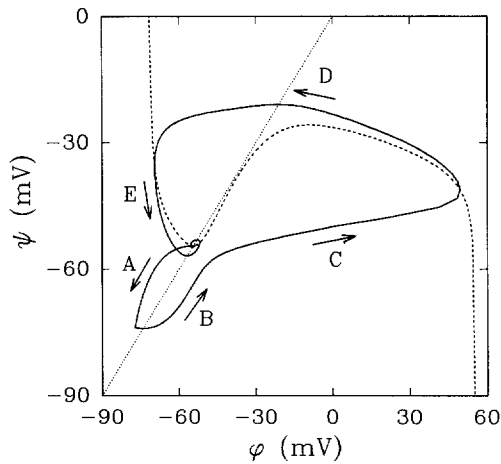


Fig. 4. The phase plane diagram of the same event as in Fig. 3 for the reduced model. The labels correspond to similar labels in Fig. 3: the V - t trajectory near the label "A" in Fig. 3 is represented by the phase-plane trajectory near the same label in this figure. The arrows give the direction of motion in the phase-plane

4 Examples: Hodgkin-Huxley, HH + I_A

A direct comparison of the full four equation Hodgkin-Huxley system with its two equation reduction is given in Fig. 3. In this figure the model neurons are hyperpolarized by injected current, and fire on rebound when the current is removed. This phenomenon, called post-inhibitory rebound (PIR), is seen in many neurons. A phase-portrait of the events shown in Fig. 3 clearly reveals the etiology of PIR. The nullclines of the phase plane indicate where the time derivatives of the dynamical variables vanish (the dotted line in Fig. 4 gives $d\psi/dt = 0$, the dashed line gives $d\phi/dt = 0$). The $d\phi/dt$ nullcline depends on the external current, but the other nullcline is always given simply by $\phi = \psi$. It is helpful to know that the rate of change of ϕ is almost everywhere significantly greater than that of ψ and to recall that ϕ

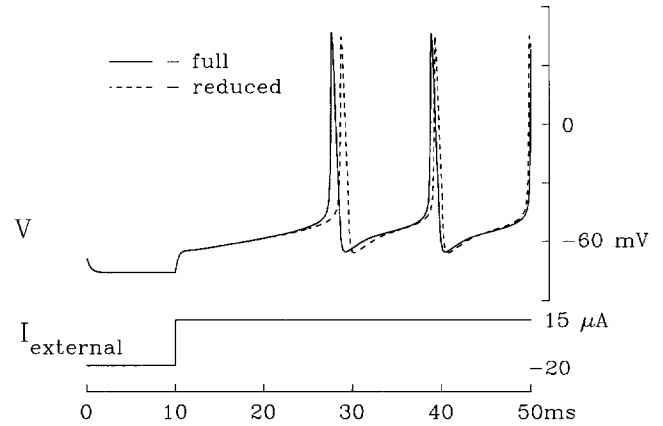


Fig. 5. Post-inhibitory latency to firing for the HH + I_A system. Hyperpolarizing current was injected for 10 ms and then switched to depolarizing current. Shown are both the full model (solid line) and the reduction (dashed line)

is the variable replacing the membrane potential V . The cell sits at rest, i.e., at the stable equilibrium point where the nullclines cross. When hyperpolarizing current is injected, the left-most lobe of the nullcline is suddenly pulled down, and the phase point moves toward its new stable equilibrium. When the hyperpolarization is released, the phase point begins to return to its original location. Before it can get there, however, it is swept into the circulatory vector field leading to the right-most arm of the nullcline. It moves leftward along the nullcline until it finally "falls off" and continues on to the left-most arm, slipping down it to finally settle back to the rest point.

A similar treatment of cells to which an I_A has been added is shown in the next pair of figures (5, 6). The full six equation system is that given by Connor et al. (1977), and the system has been reduced to three equations by combining the equivalent potential for m and the membrane potential into our ϕ as before, but now we mix the *three* equivalent potentials for h , n and a (the activation variable for I_A), to form ψ . The third variable is the equivalent potential v_b corresponding to the I_A inactivation variable b .

Figure 5 shows the voltage trace of a HH + I_A cell that is first hyperpolarized and then suddenly depolarized above threshold. Traces from both the full and

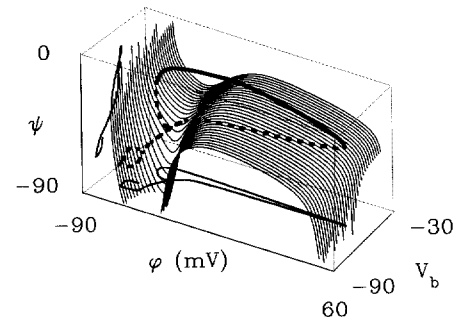


Fig. 6. Phase space portrait of the event shown in Fig. 5. The surface shown is the nullsurface $d\phi/dt = 0$. The heavy line shows the trajectory of the reduced system with the dashed line indicating a position hidden by the nullsurface. The lighter lines show the projections of this trajectory onto the coordinate planes

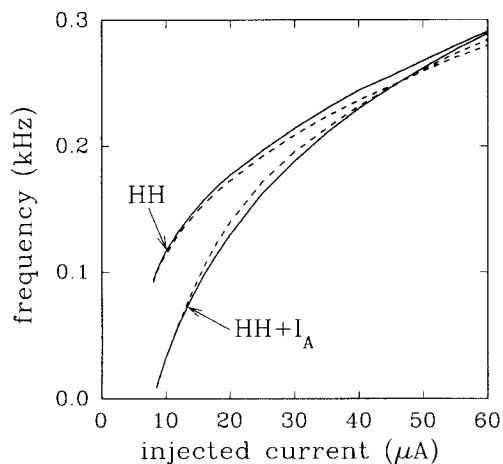


Fig. 7. Frequency vs. external current for the HH and $HH + I_A$ systems. Solid lines are for the full systems, dashed lines are for the reduced systems

reduced systems are shown superimposed. The corresponding 3-dimensional phase portrait of this event is given in Fig. 6 showing the $d\phi/dt = 0$ nullsurface (remember, the other nullclines are simply the planes $V_b = \phi$ and $\psi = \phi$), the phase trajectory and the projection of the phase trajectory onto a pair of coordinate planes. This example does not show PIR, since there is no PIR in this cell. The example instead focuses on the phenomenon of post inhibitory latency to firing. When a HH cell is depolarized sufficiently to produce firing, the onset of the first action potential is immediate and virtually independent of the degree of hyperpolarization imposed immediately beforehand. In contrast, the same cell with I_A now shows a latency to firing which depends monotonically on the potential to which it had been hyperpolarized immediately prior to depolarization. This is most clearly seen in Fig. 6: the system starts at a point “behind” the current conservation nullsurface and begins to move toward larger ϕ . Before long, however, it encounters the depression in the nullsurface. It then rides along the nullsurface toward the new equilibrium point. Motion along this portion of the

trajectory is relatively slow, since the motion is in the slow direction and motion in the fast direction is blocked. The farther down one starts, the farther one must travel along this slow path, hence the hyperpolarization-dependent delay. Before the phase point reaches its new equilibrium, it rolls off the edge of the bump in the nullsurface (where it becomes unstable) and then into the limit cycle of repetitive firing.

Figure 7 shows the firing frequency as a function of the injected current, for the full HH and $HH + I_A$ systems (solid lines) and the reduced systems (dashed lines). The reductions match the full systems quite well in both cases. As expected, the bifurcation occurs at the same place in both cases and seems to have the proper character, i.e., Hopf for HH and saddle for $HH + I_A$, though this has not been rigorously investigated.

A crucial feature of these reductions is that they preserve to a large extent the dynamic response characteristics of the original system. We have exploited the fact that all the gating variables are driven by the voltage and are otherwise uncoupled, so the reduced systems exhibit faithful behavior under dynamic as well as static conditions. This is clearly important, since physiologically relevant stimuli are rarely static, but rather highly irregular and fluctuating. Figure 8 shows the response of the $HH + I_A$ system to such an irregular (in this case, quasiperiodic) stimulus, comparing the full and reduced models. The fidelity of the reduced model is apparent.

6 Discussion

Realistic, conductance-based models can be complex and confusing. In particular, they often require a large number of dynamical variables for their description. We have provided a systematic method of reducing the complexity of these models.

The reduction scheme we have presented can be summarized by the following set of rules for reducing neuronal models:

- 1) Convert all gating variables to equivalent potentials v_i .

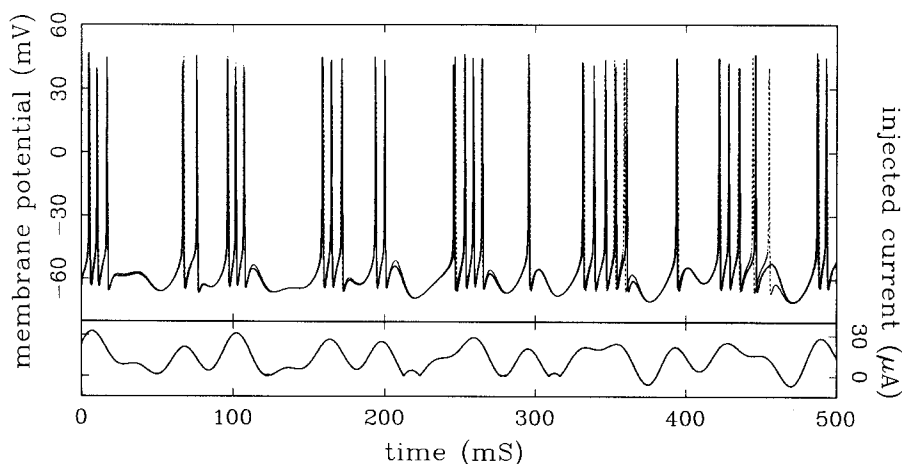


Fig. 8. Behavior of the $HH + I_A$ system under quasiperiodic current injection. The $V-t$ trajectory of the full system of six differential equations is given by the solid line while the reduction to three equations is shown dashed. All spikes in the full system have corresponding spikes in the reduced system and there is just one spike in the reduced system that has no correlate in the full system

2) Combine the membrane potential and the equivalent potentials for all gating variables satisfying $\partial F/\partial v_\mu < 0$ with rate constants satisfying (11) into the single potential φ . In the reduced model this variable replaces the membrane potential.

3) Combine the remaining equivalent potentials into one or more groups. Within a group all the rate constants k_i should be roughly the same and the derivatives $\partial F/\partial v_i$ should all have the same sign.

4) Apply (6) and (9) to determine the weighting coefficients α of the averages. The values of the α_μ for $\mu \neq 0$ are not needed.

5) Check the consistency condition, (10). If this is satisfied the reduced model is described by the equations of motion

$$C \frac{d\varphi}{dt} + \alpha_0 F(\varphi, \psi) = \alpha_0 I_{\text{external}}(t)$$

and

$$\frac{d\psi}{dt} = \sum_i \alpha_i f_i(\varphi, \psi).$$

This method uses strictly local criteria which conserve the bifurcation structure of the model. There is a simple test for consistency, informing the user when the method is likely to fail. We have shown here that this method works well for the Hodgkin–Huxley system, and the Connor et al. (1977) extension of this system. We suggest that it will be similarly useful in simplifying numerous other complex conductance-based neuronal models. These techniques may be taken as one stage in a comprehensive program of simplification in which it will be possible to generate a family of models with varying degrees of complexity from a single complex neuronal model, all related in a systematic way to each other (Abbott and Kepler 1990). This will allow formal analysis of simplified models that are derived in a coherent fashion from direct experimental results.

Acknowledgement. We wish to thank Nancy Kopell for helpful comments. This research is supported by NIH grant T32NS07292 (TBK), DOE contract DE-AC02-76ER03230 (LFA) and NIMH grant MH46742 (EM).

References

- Abbott LF, Kepler TB (1990) Model neurons: from Hodgkin–Huxley to Hopfield. In: Garrido L (ed) *Statistical mechanics of neural networks*. Springer, Berlin Heidelberg New York
- Buchholtz F, Golowasch J, Epstein IR, Marder E (1992) The contribution of individual ionic currents to the activity of a model stomatogastric ganglion neuron *J Neurophysiol* (in press)
- Connor JA, Walter D, McKown R (1977) Neural repetitive firing: modifications of the Hodgkin–Huxley axon suggested by experimental results from crustacean axons. *Biophys J* 18: 81–102
- FitzHugh R (1961) Impulses and physiological states in models of nerve membrane. *Biophys J* 1:445–466
- Golowasch J, Buchholtz F, Epstein IR, Marder E (1992) A mathematical model of an identified stomatogastric ganglion neuron *J Neurophysiol* (in press)
- Hindmarsh JL, Rose RM (1982) A model of the nerve impulse using two first-order differential equations. *Nature* 296: 162–164
- Hodgkin AL, Huxley AF (1952) A quantitative description of membrane current and its application to conduction and excitation in nerve. *J Physiol* 117:500
- Hopfield JJ (1982) Neural networks and physical systems with emergent collective computational abilities. *Proc Natl Acad Sci* 79:2554
- Krinskii VI and Kokoz YM (1973) Analysis of equations of excitable membranes – 1. Reduction of the Hodgkin–Huxley equations to a second-order system. *Biofizika* 18:506–511
- Lapicque L (1907) Recherches quantitatives sur l'excitation électrique des nerfs traitée comme une polarisation. *J Physiol Pathol Gen* 9:620–635
- McCulloch WS, Pitts W (1943) A logical calculus of the ideas immanent in nervous activity. *Bull Math Biophys* 5:114–133
- Rinzel J (1985) Excitation dynamics: insights from simplified membrane models. *Fed Proc* 44:2944–2946
- Rose RM, Hindmarsh JL (1989) The assembly of ionic currents in a thalamic neuron I. The three-dimensional model. *Proc R Soc Lond* 237:267
- Yamada WM, Koch C, Adams PR (1989) Multiple channels and calcium dynamics. In *Methods of neuronal modeling* In: Koch C, Segev I (eds) *From synapses to networks*. MIT Press, Cambridge

Dr Thomas B. Kepler
 Santa Fe Institute
 1660 Old Pecos Trail
 Santa Fe, NM 87501
 USA
 FAX (1) 505–9820565